Intelligent Control in Current Digital Switching Power Amplifier for Active Magnetic Bearing

Jun Wang, Mingzhe Zou, Maocheng Zhao and Cong Huang

School of Information Science and Technology,
Nanjing Forestry University, Nanjing 210037, Jiangsu, China

Abstract
To effectively reduce the influence of high power loss and low reliability caused by fixed supply voltage for current switching power amplifier, a new and simple circuit with intelligent control is proposed in this paper. The digital control strategy of minimum switching frequency is adopted and the DC power supply voltage is changed by regulating actively single phase half controlled bridge rectifier circuit. Theoretical analysis of intelligent control and model analysis of circuit are derived in detail. Compared with the simulation and experiment, the results show that the characteristics of the ripple voltage, steady state and dynamic state are basically consistent. Power supply voltage can be successfully changed by actively tracking the actual load current and adjusted in real time. The power loss is reduced to a maximum of 33.9%. These results indicate that the proposed strategy is feasible and effective for power amplifier circuit.
Key words: INTELLIGENT CONTROL, SWITCHING POWER AMPLIFIER, ACTIVE MAGNETIC BEARING

1. Introduction

Active magnetic bearing is a kind of high technology equipment with the integration of mechanical and electrical [1-3]. It has been applied to different industrial areas, such as high speed motor, artificial heart pump, centrifugal compressor and flywheel energy storage [4-8]. Because the traditional mechanical rolling bearings and other the structural complexity of the lubrication system are eliminated in active magnetic bearings, it has less volume and weight [9-11]. At the same time, it brings to improve safety and reliability.

In active magnetic bearing system, the levitation force is realized by adjusting the current of the magnetic coil of the radial and axial bearing. In the process of bearing high speed operation, the current of the electromagnetic coil can be actively adjusted according to the position of the rotor in real time [12-14]. So the current power amplifier is one of the key technologies of active magnetic bearing system. In order to improve the efficiency and band width of power amplifier, two level and three level switching mode power amplifier were proposed [15]. According to the switching circuit theory, Wang et al. established the mathematical model of the circuit [16]. They concluded that three-level switching power amplifier has the advantages of the low switching loss and small current ripple compared to the two level switching power amplifier from the results of software simulation and experimental verification[17]. So three-level switching

power amplifier is widely used at present. Wang et al. used pulse width modulation (PWM) method of bipolar triangular wave to control three-level amplifier [18]. Park had designed two-way digital power amplifier using DSP processor and applied to the system of magnetic bearing wheels [19]. Chen et al. used personal computer (PC) as the control core and control 5 freedom degree of magnetic bearing system [20]. In these studies, DC power supply voltages used in power amplifier are fixed. If the supply voltage is low, the power amplifier cannot meet the needs of the dynamic changes of the load when the rotor is running at high speed. On the contrary, if the voltage is high enough to real-time dynamic adjustment, but the power device is easy to damage and increase power consumption.

The purpose of this paper is to research the intelligent control for unipolar three-level digital switching power amplifier. The digital control strategy of minimum switching frequency is achieved by single chip microcomputer. The DC power supply voltage is changed by actively tracking the actual load current and adjusted in real time. The proposed circuit can meet the requirements of the current power amplifier for the dynamic response with the current change and improve the utilization of power supply.

2. Intelligent control principle for unipolar three-level digital switching power amplifier

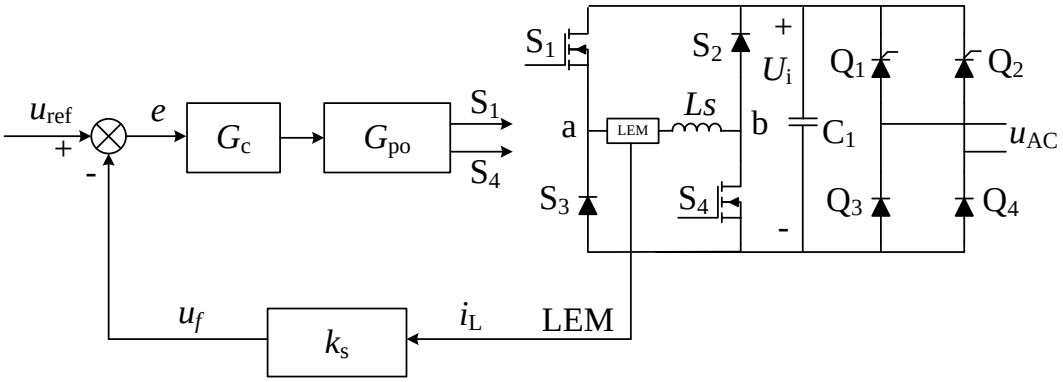

Figure 1. Intelligent control schematic of three-level current mode switching power amplifier

2.1 Circuit structure

The intelligent control schematic of three level current mode switching power amplifier is shown in Figure 1. The system mainly includes a digital error controller, a digital pulse width generator, a current feedback loop, a unipolar bridge converter and a single phase half controlled bridge rectifier circuit. Digital error controller G_c is adopted discrete proportional-integral algorithm, K_s is the current-voltage transfer coefficient of feedback loop, G_{po} is the magnification of pulse width generator, LEM is the current sensor, L_s is the nominal equivalent inductance values of the electromagnetic coils. MOSFETs S_1, S_4 and fast recovery diodes S_2, S_3 comprise the unipolar bridge converter. Thyristors Q_1, Q_2 and rectifier diodes Q_3, Q_4 comprise the single phase half controlled bridge rectifier circuit. U_i is the rectifier DC bus voltage. C_1 is the DC filter capacitor.

2.2 Theoretical analysis of intelligent control

The unipolar bridge converter is operating in continuous current mode, in which the bias currents are set at half of the maximum allowable current. The control current is added to the bias current in magnetic bearing coils. This mode can provide maximum force dynamic characteristics and good linearity of the control current.

2.2.1 Digital control strategy for the minimum number of switches

For reducing the complicated hardware resources which are convenient for some industrial applications with high reliability and small size, the digital microcontroller is designed to simultaneously calculate the function of the current conversion for LEM loop, digital error controller and pulse width generator loop. AD module inside the microcontroller is responsible for the current feedback signal sampling. AD module is a 10-

bit converter and its acquisition is achieved through an internal eight channel selector. The interrupt mode is adopted in AD program. The error is recalculated when sampling of one cycle is completed for every time. Two ways with 16-bit PCA module have the same time reference. They use the alignment methods of rising edge to output two channel PWM signals, respectively for driving power MOSFET S_1 and S_4. PCA module has a comparison register and a 16 bit counter. Comparison register is loaded the voltage error and counter starts counting from 0 at each switching cycle. If the count value is less than the comparison register value, the port of PCA module outputs high level of 1, otherwise the corresponding port outputs low level of 0. In this way, it is only needed to change the value of the comparison register in software program and the single chip microcomputer can generate the corresponding PWM wave. The error controller is used to operate the discrete PI control algorithm. Because discrete digital signals are often used in the single chip microcomputer, the voltage error is calculated in a sampling period by PI discrete transfer function as follow

$$\frac{u_k - u_{k-1}}{T} = k_p\left[\frac{e_k - e_{k-1}}{T} + \frac{e_k}{T_i}\right] \quad (1)$$

Where, u_k is current voltage, e_k is the sampling error of the current period, u_{k-1} is the voltage of last period, e_{k-1} is the sampling error of the last period, T is the sampling interval period. T_i is integral time coefficient, k_p is proportional coefficient.

The transfer function of discrete controller based on incremental PI algorithm is derived by transformation of Formula (1).

$$\Delta u = k_p\left[\left(e_k - e_{k-1}\right) + \frac{T}{T_i}e_k\right] \quad (2)$$

Where, $\Delta u = u_k - u_{k-1}$.

The operational register in the single chip microcomputer has only 8 bit and its maximum value is 255. So it is necessary to limit the output of the discrete error Δu in order to prevent load current overload which causes damage to circuit and power devices, and even reduces system instability.

2.2.2 Dynamic behavior modeling of current mode switching power amplifier

The control dynamic behavior by applying minimum switching frequency is analyzed in this section. In one switching period, there have only two circuit operating modes for the unipolar bridge three level converter. Figure 2 shows the PWM drive and load current waveform in current-rise and current-decrease state respectively. For current-rise state, MOSFET S_1 is always on when the actual load current is less than the given reference current. So if the MOSFET S_4 is on, the circuit is in the charging mode and the load current rises up. If the MOSFET S_4 is off, the circuit is in the freewheeling mode and the load current almost remains unchanged. The circuit equations based on Kirchhoff Voltage Law (KVL) are obtained as below:

$$L_s\frac{\mathrm{d}i_L(t)}{\mathrm{d}t} + ri_L(t) = U_{\text{in}} - 2U_{\text{on}} \quad (3)$$

$$L_s\frac{\mathrm{d}i_L(t)}{\mathrm{d}t} + ri_L(t) = -U_{\text{on}} - U_{\text{D}} \quad (4)$$

Where i_L is the inductor current, r is the resistor of inductor coil, U_{on} is the conducting voltage of switching devices. U_D is the forward voltage of diodes.

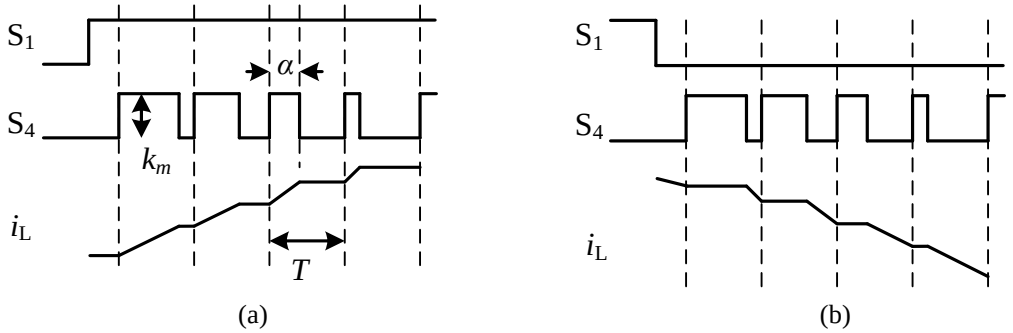

(a) (b)

Figure 2. The PWM drive and load current waveform in current-rise and current-decrease state. (a) current-rise state. (b) current-rise state

For current-decrease state, the actual load current is greater than the given reference current and MOSFET S_1 is always off. So if the MOSFET S_4 is on, the circuit is in the freewheeling mode and the load current almost remains unchanged. If the MOSFET S_4 is off,

the circuit is in the discharging mode and the load current is decreased. The circuit equations can be described as

$$L_s \frac{\mathrm{d}i_L(t)}{\mathrm{d}t} + ri_L(t) = -U_{\text{on}} - U_{\text{D}} \quad (5)$$

$$L_s \frac{\mathrm{d}i_L(t)}{\mathrm{d}t} + ri_L(t) = -U_{\text{in}} - 2U_{\text{D}} \quad (6)$$

For each PWM period, the three level current power amplifier mainly works in current-rise state. The amount of current rise and the amount of the current fall are equal because of the inductive charge and discharge energy conservation. Therefore, according to the formula (3) and (4), the relationship between the current ripple under digital control strategy with the minimum number of switches can be expressed as

$$\Delta i_L = \frac{U_{\text{on}} + U_{\text{D}} + ri_0}{2 f_s L_s} \quad (7)$$

From the formula (7), we have the conclusion that the ripple of three level current power amplifier with this proposed method is the same as the traditional power amplifier with PWM pulse width modulation. The current of new digital circuit also has the advantages of small ripple and does not change with voltage U_{i}.

2.2.3 Steady state model of new power amplifier

According to figure 2, the relationship between the error and the period can be described as

$$e = \frac{k_m \alpha}{T} \quad (8)$$

The relationship between the voltage in the middle of the bridge circuit and the DC voltage U_{i} is written as

$$U_{ab} = \frac{\alpha}{T} U_i \quad (9)$$

The mathematical model between the load current and the reference input voltage is simplified as

$$G_{\text{model}} = \frac{k_p U_i s + k_I U_i}{k_m L_s s^2 + \left(r k_m + k_s k_p U_i\right) s + k_s k_I U_i} \quad (10)$$

2.2.4 Analysis of single phase half controlled bridge rectifier circuit

The role of single phase bridge half controlled rectifier circuit is to supply a variable DC supply voltage for switching power amplifier. The load of power amplifier is the electromagnetic coils. Coil resistance is usually few ohms. Therefore the electromagnetic coil can be considered that it is basically equivalent to an inductance. The object of the current response speed is that the output of the actual current can be as far as possible track input control signal without the distortion. Neglecting the voltage drops of resistance and power devices, the current is assumed as a sinusoidal desired signal of $I = I_{\text{m}}\text{Sin}\omega t$. The current response of the load coil is required to meet the following conditions:

$$\left|\frac{dI}{dt}\right|_{\max} = I_m \omega \le \frac{u_{\text{i}}}{L_s} \quad (11)$$

The above equation can be simplified as

$$u_{\text{i}} \ge I_m \omega L_s \quad (12)$$

This above criterion puts a limit on the minimum supply voltage. That is, good dynamic characteristics of power amplifier for magnetic bearing in high rotor speed support are feasible by promoting the supply voltage.

Figure 3 shows schematic analysis of single phase half controlled bridge rectifier circuit. From the equivalent circuit diagram of Figure 3(a), the load current is continuous in a switching period, but the power amplifier can be obtained current from the DC link voltage only in the charging time. The current of single phase bridge half controlled rectifier circuit is provided for power amplifier as

$$I_{IN} = I_{Ls} \cdot \Delta t / T \quad (13)$$

During the time of t_{c}, the filter capacitor C_1 is charged. The voltage variation is basically the same as the input voltage u_{AC}. The charging voltage equation of the capacitor is written as

$$u_t = \sqrt{2} U_{AC} \sin 2\pi f t \quad (14)$$

Assume that the ripple voltage is ΔU, then the minimum voltage is described as

$$U_{\min} = \sqrt{2} U_{AC} \sin 2\pi f t_1 = U_{\max} - \Delta U \quad (15)$$

Then, the time of charging to filter capacitor is deduced as

$$t_c = \frac{1}{2\pi f}\left(\arcsin\frac{U_{\max}}{\sqrt{2}U_{AC}} - \arcsin\frac{U_{\max} - \Delta U}{\sqrt{2}U_{AC}}\right) \quad (16)$$

During the time of t_{f}, the filter capacitor C_1 is discharged. The load of bridge rectifier circuit is the current I_{in}. So it is equivalent to a constant current source. The time of discharging to filter capacitor is deduced as

$$t_f = C_1 \frac{\Delta U}{I_{IN}} \quad (17)$$

Substituting (17) into (15) and (16), we have the relationship of voltage ripple, filter capacitor and current of the power amplifier as follow

$$\frac{1}{2\pi f}\left(\arcsin\frac{U_{\max}}{\sqrt{2}U_{AC}} - \arcsin\frac{U_{\max}-\Delta U}{\sqrt{2}U_{AC}}\right) + C_1\frac{\Delta U}{I_{IN}} = \frac{T_{AC}}{2} \quad (18)$$

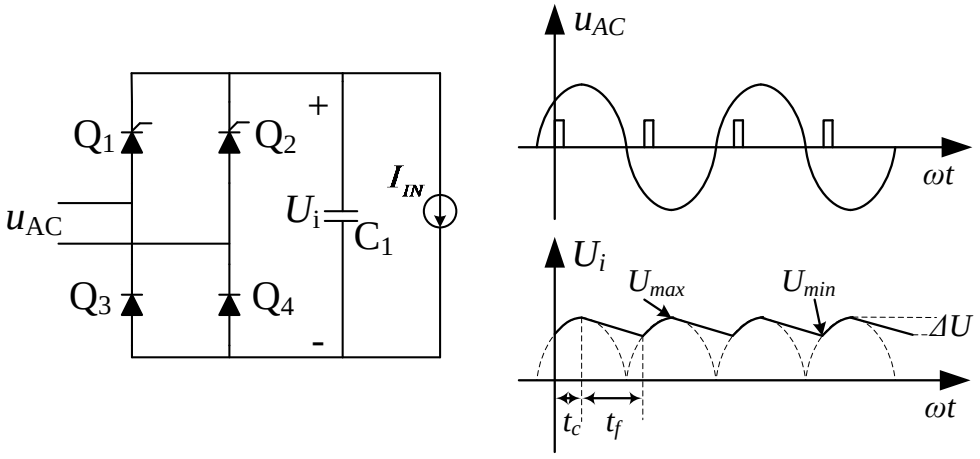

(a) (b)

Figure 3. Schematic analysis of single phase half controlled bridge rectifier circuit.(a) Equivalent circuit diagram. (b) Circuit working principle.

3. Simulation Results and Discussion

In this section, simulations are carried out for the verification analysis of intelligent control in three level current mode switching power amplifier. By considering the circuit in the ideal operation condition, the parasitic parameters of the devices are ignored. Simulation parameters are U_{AC}=120V, T_{AC}=50Hz, h=1, L_s=1.75mH, C_1=470uF.

Simulation current and voltage waveforms under steady state conditions of the proposed circuit are shown in Figure 4. i_L is the current in coil and U_i is the voltage in capacitor C_1. The steady state current of the electromagnetic coils is approximately 2.43A. Because the current rate of the coil is zero, the minimum voltage of 31V is provided to overcome the voltage drop of the circuit devices such as the coil resistance and power switching modules. As mentioned in the preceding theoretical analysis, the voltage has ripple of about 5V. But the ripple does not affect the normal operation of the switching power amplifier. Figure 5 shows the simulation current and voltage waveforms when the frequency of 200Hz. The AC amplitude of the coil current is 1A. According to the calculation of formula (12), the DC voltage is adjusted to 70V in order to guarantee sufficient current response rate.

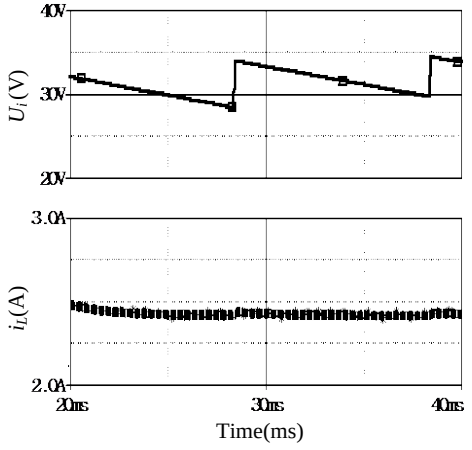

Figure 4. Simulation current and voltage waveforms under steady state conditions

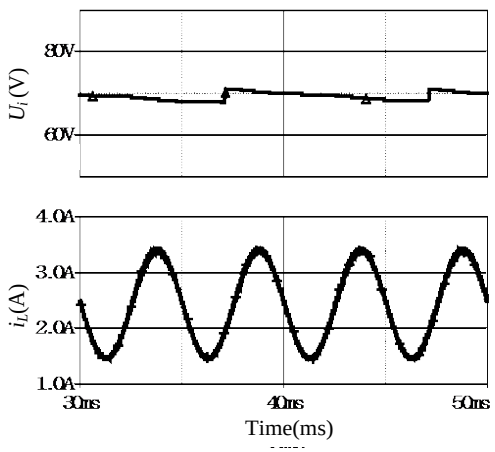

Figure 5. Simulation current and voltage waveforms when the frequency of 200Hz

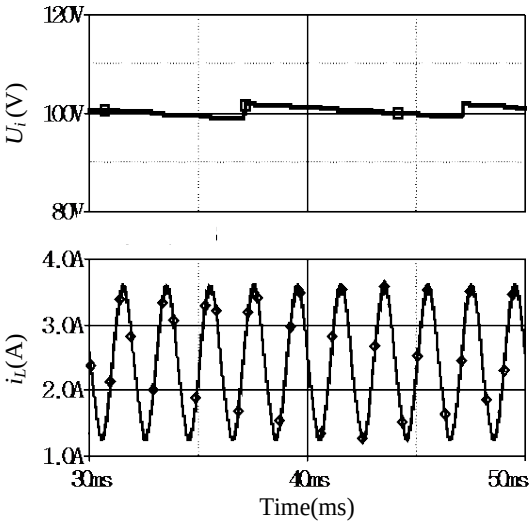

Figure 6. Simulation current and voltage waveforms when the frequency of 500Hz

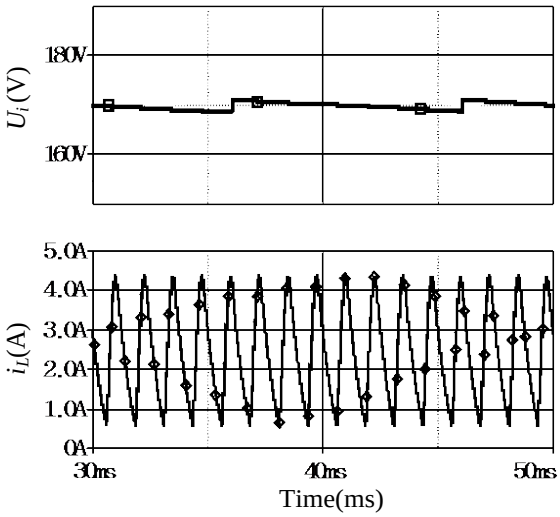

Figure 7. Simulation current and voltage waveforms when the frequency of 800Hz

Simulation current and voltage waveforms when the frequency of 500Hz are shown in Figure 6. The frequency of the coil current can actually reflect the operating speed of the rotor of magnetic bearing system. The higher the frequency is, the faster the rotor system is running. The amplitude of the coil current is about 1.2A. The DC voltage corresponds to rise up to 100V by the circuit active control. Figure 7 shows the simulation current and voltage waveforms when the frequency of 800Hz. The current amplitude is reached 2A, which is close to the maximum range of allowable current. At this time, the maximum value of the DC voltage is 170V which is reached to the peak value of the AC input voltage. From these simulation waveforms of the voltage, the voltage is changed periodically at 10ms per cycle.

4. Experimental Results and Discussion

In this section, experiments are carried out to verify the previous theory model and simulation analysis. In the actual circuit, the types of MOSFET S_1 and S_4 are IRFP460 and the types of fast recovery diodes S_2 and S_3 are MUR860. The types of thyristors Q_1 and Q_2 are CS30 and the types of rectifier diodes Q_3 and Q_4 are VS40. The coil current is detected in real time by using hall current sensor in the experiments. The following figures are obtained according to the data captured by Tektronix digital oscilloscope DPO2024 and current probe TCP202.

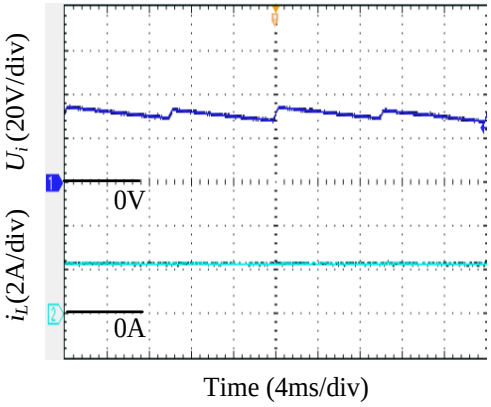

Figure 8. Experimental current and voltage waveforms under steady state conditions

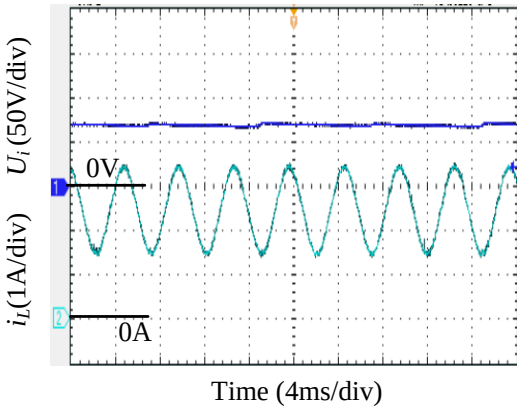

Figure 9. Experimental current and voltage waveforms when the frequency of 200Hz

Figure 8 shows the experimental current and voltage waveforms under steady state conditions. The load current generated by the digital current power amplifier is 2.4A, which the error compared with the simulation data is 1.25%. The average direct current

voltage is 30V. The period of ripple voltage is 10ms and the amplitude is 5V, which are the same as the simulation values.

Figure 9 shows the experimental current and voltage waveforms when the frequency of 200Hz. The actual peak to peak current is 2A and the average voltage is up to 70V. When the frequency of current is at 500Hz and 800Hz, experimental current and voltage waveforms are shown in Figure 10 and Figure 11. In the process of high speed operation of magnetic bearing system, the current amplitude in the dynamic adjustment is easy to become larger because the rotor is needed to be suspended in the center state. The peak current is 2.4A at 500Hz. With the increase of current amplitude and frequency, the power amplifier needs a higher DC voltage to offset the impact of the parameters change. So the actual voltage of filter capacitor is raised to 100V. Similarly, if the frequency is above 800Hz and the amplitude exceeds 4.8A, the maximum value of the rectified DC voltage reaches to 170V and remains unchanged.

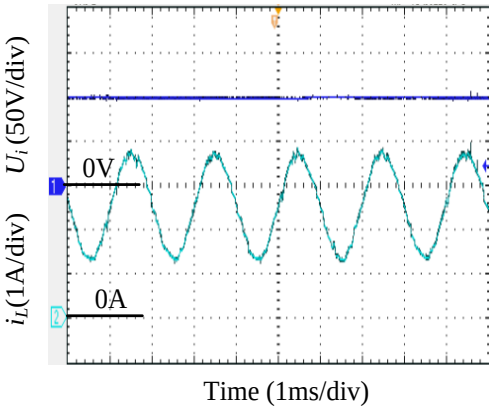

Figure 10. Experimental current and voltage waveforms when the frequency of 500Hz

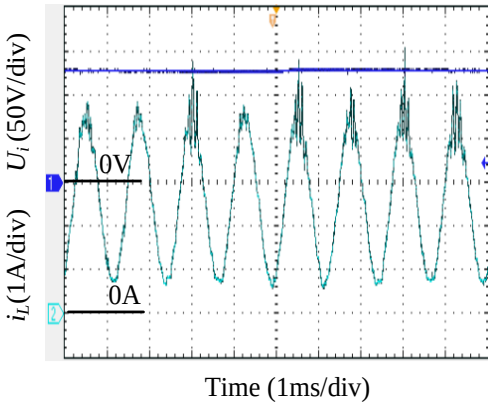

Figure 11. Experimental current and voltage waveforms when the frequency of 800Hz

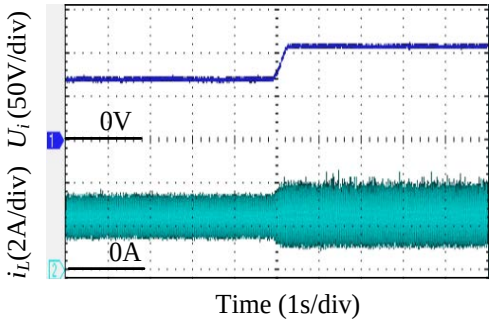

Figure 12. Experimental current and voltage waveforms when the magnitude of the current transition

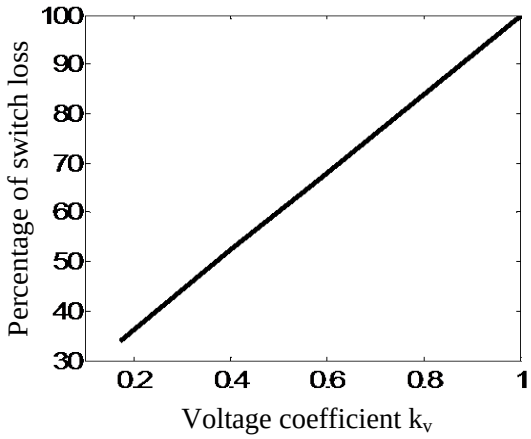

Figure 13. Relationship between percentage of switch loss and voltage coefficient

In order to verify the current digital power amplifier can be realized automatically to control voltage, experimental current and voltage waveforms when the magnitude of the current transition are shown in Figure 12. At present, the initial current is the peak to peak amplitude of 2A and the initial voltage is 70V. The current is suddenly jumped to 3A, then the voltage is quickly adjusted to 110V by digital power amplifier. The delayed response time is about 200ms and the rotor system of magnetic bearing can run normally.

Figure 13 shows the relationship between percentage of switch loss and voltage coefficient. Percentage of switch loss is described as the ratio of the loss with using the proposed circuit and the loss with traditional power amplifier. Voltage coefficient is described as the ratio of rectified DC

voltage adopted the proposed circuit and the voltage with traditional circuit. For example, the switch loss without proposed circuit is 28.8W in the case of the DC voltage 170V and average current 2.4A. After adopting the proposed circuit, the average current remains 2.4A but the voltage drops to 30V. The switch loss adopted proposed circuit is 9.79W. So voltage coefficient is 0.176 and percentage of switch loss is 33.9%. From that we can see that the new digital power amplifier can greatly reduce the switching loss and improve the efficiency of the circuit system.

5. Conclusions

This proposed circuit works by substitution of the fixed power supply voltage by adopting intelligent controlled bridge rectifier circuit. Compared with the traditional PWM modulation, the proposed solution has made the DC power supply voltage to change by actively tracking the actual load current and adjusted in real time. The presented circuit has been verified by experiment results. Moreover, it can effectively reduce the power loss and improve the utilization of power supply. Taking these into account, this new technique is both simple and effective for widely high speed applications of active magnetic bearing used in many industrial fields.

Acknowledgements

This work was supported by National Nature Science Foundation of China (Grant No. 51275240), the Natural Science Foundation of the Jiangsu Higher Education Institutions of China(Grant No.13KJB510014), the Enterprise Doctor Gathering Plan of Jiangsu Province (Grant No.2012165) and the Practice Innovation Training Program Project of the Jiangsu College Students(Grant No. 201410298028Z).

References

1. Barbaraci G, Mariotti G.V., Piscopo A. (2013) Active Magnetic Bearing Design Study. *Journal of Vibration and Control*, 19(16), p.p. 2491-2505.
2. Looser A., Kolar J.(2014) An Active Magnetic Damper Concept for Stabilization of Gas-bearings in High-speed Permanent Magnet Machines. *IEEE Transcations on Industrial Eletronics*, 61, p.p. 3089-3098.
3. Tiwari R., Chougale A. (2014) Identification of Bearing Dynamic Parameters and Unbalance States in a Flexible Rotor System Fully Levitated on Active Magnetic Bearings. *Mechatronics*, 24(3), p.p. 274-286.
4. Grabner H., Amrhein W., Silber S., Gruber W. (2010) Nonlinear Feedback Control of A Bearing Brushless DC Motor, *IEEE/ASME Transcations Mechatronics*, 15(1), p.p.40-47.
5. Zhang S., Luo F.L. (2009) Direct Control of Radial Displacement for Bearingless Permanent Magnet Type Synchronous Motors, *IEEE Transcations on Industrial Eletronics*, 56(2), p.p.542-552.
6. Tera T., Yamauchi Y., Chiba A., Fukao T., Rahman M.A. (2006) Performances of Bearingless and Sensorless Induction Motor Drive based on Mutual Inductances and Rotor Displacements Estimation, *IEEE Transcations on Industrial Eletronics*, 53(1), p.p.187-194.
7. Yang S.M., Huang M.S. (2009) Design and Implementation of a Magnetically Levitated Single-axis Controlled Axial Blood Pump, *IEEE Transcations on Industrial Eletronics*, 56(6), p.p.2213-2219.
8. Yu L.H., Fang J.C., Wu C. (2005) Magnetically Suspended Control Gyrogimbal Servo-system using Adaptive Inverse Control during Disturbances, *Electronics Letters*, 41(17), p.p.950-951.
9. Saeed N.A., Eissa, Eissa M., ElGanini W.A. (2013) Nonlinear Oscillations of Rotor Active Magnetic Bearings System. *Nonlinear Dynamics*, 74(1), p.p.1-20.
10. Zhong Z. X., Zhu C. S. (2013) Vibration of Flexible Rotor Systems with Two-degree-of-freedom PID Controller of Active Magnetic Bearings. *Journal of Vibroengineering*, 15(3), p.p.1302-1310.
11. Radhakrishna M., Jana S., Sreedhar B.K., Kalyanasundaram P., Kumar V.A. (2013) Development of Active Magnetic Bearings for a Vertical Centrifugal Pump Rotor. *Advances in Vibration Engineering*, 12(4), p.p.329-335.
12. Fang J.C., Ren Y. (2012) Self-Adaptive Phase-Lead Compensation Based on Unsymmetrical Current Sampling Resistance Network for Magnetic Bearing Switching Power Amplifiers. *IEEE Transactions on Industrial Electronics*, 59(2), p.p. 1218-1227.
13. Ren Y., Fang J.C. (2012) Current-sensing Resistor Design to Include Current Derivative in PWM H-bridge Unipolar Switching Power Amplifiers for Magnetic Bearings. *IEEE Transactions on Industrial Electronics*, 59(12), p.p. 4590-4600.
14. Fan Y.P., Liu S.Q., Li H.W. (2013) Time Delay Compensation of Switching Power Amplifier for Magnetic Bearing based on DOB. *Electric Machines and Control*, 17(5), p.p. 103-109.

15. Yu W.T., Fan Y.P., Liu S.Q. (2010) Research on MATLAB Simulation of Three Level Power Amplifier for Magnetic Bearings. *Proc. Conf. on Power and Energy Engineering*, Chengdu, China, p.p.1-4.
16. Wang J., Xu L.X. (2009) Analysis and Modeling of a Switching Power Amplifier for Magnetic Bearing. *Proc. Conf. on the 4th IEEE Industrial Electronics and Applications*, Xi'an, China, p.p. 2257-2261.
17. Ji L., Xu L., Jin C. (2013) Research on a Low Power Consumption Six-Pole Heteropolar Hybrid Magnetic Bearing. *IEEE Transactions on Magnetics*, 49(8), p.p. 4918-4926.
18. Wang J., Wang L.P., Dong J.H., Huang C. (2015) Research on the Steady State and Ripple Current Models of Current Mode Switching Power Amplifier for Magnetic Bearing. *Journal of Software Engineering*, 9(1), p.p.157-168.
19. Park Y. (2014) Design and Implementation of an Electromagnetic Levitation System for Active Magnetic Bearing Wheels. *IET Control Theory Applications*, 8(2), p.p. 139-148.
20. Chen S.Y., Lin F.J. (2013) Decentralized PID Neural Network Control for Five Degree-of-freedom Active Magnetic Bearing. *Engineering Applications of Artificial Intelligence*, 26, p.p. 962-973.